SUPPLEMENT TO "ON THE FACTOR STRUCTURE OF BOND RETURNS"

RICHARD K. CRUMP
Federal Reserve Bank of New York

NIKOLAY GOSPODINOV
Federal Reserve Bank of Atlanta

APPENDIX B: BOUNDS ON EIGENVALUES AND EIGENVECTORS

IN THIS APPENDIX, WE PROVIDE bounds on the eigenvalues of V_D given in Lemma 2 in the paper based on a modification of the approach in Ipsen and Nadler (2009). To do so, we apply the bounding approach of Ipsen and Nadler (2009) to both V_D^{-1} and V_D and combine these bounds. First, we may directly apply the results in Ipsen and Nadler (2009) to V_D using the relation $V_D = \tilde{V}_D - \varkappa\varkappa'$ and the eigendecomposition of $\tilde{V}_D$ given in Lemma 2 in the paper. Let us define $h_{\lambda,n} = \lambda_{n-1} - \lambda_n$ and $\tilde{\varkappa}_{a:b} = [\psi_a \ \psi_{a+1} \ \cdots \ \psi_{b-1} \ \psi_b]'\varkappa$ for integers $a \leq b$. Then, for the interior eigenvalues ($\phi_2, \phi_3, \ldots, \phi_{N-1}$), we have the bounds

$$\phi_{n,L}(\lambda) = \max\left\{\lambda_{n+1}, \lambda_n + \frac{1}{2}\left(h_{\lambda,n} - \|\tilde{\varkappa}_{1:n}\|^2 - \sqrt{\left(h_{\lambda,n} - \|\tilde{\varkappa}_{1:n}\|^2\right)^2 + 4h_{\lambda,n}|\tilde{\varkappa}_{n:n}|^2}\right)\right\},$$

$$\phi_{n,U}(\lambda) = \lambda_n + \frac{1}{2}\left(-h_{\lambda,n+1} - \|\tilde{\varkappa}_{n:N}\|^2 + \sqrt{\left(h_{\lambda,n+1} - \|\tilde{\varkappa}_{n:N}\|^2\right)^2 + 4h_{\lambda,n+1}\|\tilde{\varkappa}_{n+1:N}\|^2}\right).$$

For the smallest eigenvalue, ϕ_N, we have the bounds

$$\phi_{N,L}(\lambda) = \lambda_N + \frac{1}{2}\left(h_{\lambda,N} - \|\varkappa\|^2 - \sqrt{\left(h_{\lambda,N} - \|\varkappa\|^2\right)^2 + 4h_{\lambda,N}|\tilde{\varkappa}_{N:N}|^2}\right),$$

$$\phi_{N,U}(\lambda) = \lambda_N + \frac{1}{2}\left(h_{\lambda,N} - \|\tilde{\varkappa}_{N-1:N}\|^2 - \sqrt{\left(h_{\lambda,N} - \|\tilde{\varkappa}_{N-1:N}\|^2\right)^2 + 4h_{\lambda,N}|\tilde{\varkappa}_{N:N}|^2}\right).$$

For the largest eigenvalue, ϕ_1, we have the bounds

$$\phi_{1,L}(\lambda) = \lambda_1 + \frac{1}{2}\left(-h_{\lambda,2} - \|\tilde{\varkappa}_{1:2}\|^2 + \sqrt{\left(h_{\lambda,2} - \|\tilde{\varkappa}_{1:2}\|^2\right)^2 + 4h_{\lambda,2}|\tilde{\varkappa}_{2:2}|^2}\right),$$

$$\phi_{1,U}(\lambda) = \lambda_1 + \frac{1}{2}\left(-h_{\lambda,2} - \|\varkappa\|^2 + \sqrt{\left(h_{\lambda,2} - \|\varkappa\|^2\right)^2 + 4h_{\lambda,2}\|\tilde{\varkappa}_{2:N}\|^2}\right).$$

Next, we will obtain bounds on the eigenvalues of V_D^{-1} using the relation $V_D^{-1} = \tilde{V}_D^{-1} + xx'$ and the eigendecomposition of $\tilde{V}_D^{-1}$. Let us first define the eigenvalues of $\tilde{V}_D^{-1}$ as

$$\ell_n = \frac{1 + \rho^2 + 2\rho\cos\left(\dfrac{2n\pi}{2N+1}\right)}{\sigma^2}, \quad n = 1, \ldots, N$$

Richard K. Crump: richard.crump@ny.frb.org
Nikolay Gospodinov: nikolay.gospodinov@atl.frb.org

and notice that $\ell_1 > \ell_2 > \cdots > \ell_N$ (i.e., $\lambda_n^{-1} = \ell_{N-n+1}$). Also, let us define the gap between adjacent eigenvalues as

$$h_{\ell,n} = \ell_{n-1} - \ell_n = \frac{4\rho}{\sigma^2} \sin\left(\frac{(2n-1)\pi}{2N+1}\right) \sin\left(\frac{\pi}{2N+1}\right).$$

Next, define $\tilde{x}_{a:b} = [\psi_{N-a+1} \ \psi_{N+a} \ \cdots \ \psi_{N-b-1}]'x$. Then, for the interior eigenvalues (ϕ_2, $\phi_3, \ldots, \phi_{N-1}$), we have the bounds

$$\phi_{N-n+1,L}(\ell)^{-1} = \min\left\{\ell_{n-1}, \ell_n + \frac{1}{2}\left(-h_{\ell,n+1} + \|\tilde{x}_{n:N}\|^2\right.\right.$$

$$\left.\left. + \sqrt{\left(h_{\ell,n+1} + \|\tilde{x}_{n:N}\|^2\right)^2 - 4h_{\ell,n+1}|\tilde{x}_{n+1:N}|^2}\right)\right\},$$

$$\phi_{N-n+1,U}(\ell)^{-1} = \ell_n + \frac{1}{2}\left(h_{\ell,n} + \|\tilde{x}_{1:n}\|^2 - \sqrt{\left(h_{\ell,n} + \|\tilde{x}_{1:n}\|^2\right)^2 - 4h_{\ell,n}\|\tilde{x}_{n:n}\|^2}\right).$$

Similarly, for the largest eigenvalue of V_D, we have

$$\phi_{1,L}(\ell)^{-1} = \ell_N + \frac{1}{2}\left(h_{\ell,N} + \|\tilde{x}_{N-1:N}\|^2 - \sqrt{\left(h_{\ell,N} + \|\tilde{x}_{N-1:N}\|^2\right)^2 - 4h_{\ell,N}|\tilde{x}_{N:N}|^2}\right),$$

$$\phi_{1,U}(\ell)^{-1} = \ell_N + \frac{1}{2}\left(h_{\ell,N} - \|x\|^2 - \sqrt{\left(h_{\ell,N} + \|x\|^2\right)^2 - 4h_{\ell,N}|\tilde{x}_{N:N}|^2}\right),$$

and for the smallest eigenvalue of V_D, we have

$$\phi_{N,L}(\ell)^{-1} = \ell_1 + \frac{1}{2}\left(-h_{\ell,2} + \|x\|^2 + \sqrt{\left(h_{\ell,2} + \|x\|^2\right)^2 - 4h_{\ell,2}|\tilde{x}_{2:N}|^2}\right),$$

$$\phi_{N,U}(\ell)^{-1} = \ell_1 + \frac{1}{2}\left(-h_{\ell,2} + \|\tilde{x}_{1:2}\|^2 + \sqrt{\left(h_{\ell,2} + \|\tilde{x}_{1:2}\|^2\right)^2 - 4h_{\ell,2}\|\tilde{x}_{2:2}\|^2}\right).$$

Finally, we may combine bounds by choosing the least upper bound and largest lower bound,

$$\max\{\phi_{n,L}(\ell), \phi_{n,L}(\lambda)\} \leq \phi_n \leq \min\{\phi_{n,U}(\ell), \phi_{n,U}(\lambda)\},$$

which improves upon the bounds given directly in Ipsen and Nadler (2009). As an example, consider $\rho = 0.99$ and $N = 20$ as used in the text. Then, the lower bound, true eigenvalues, and upper bound for $n = 1, \ldots, 5$ are, respectively: {146.1988, 146.2077, 146.2086}, {18.8180, 18.8197, 18.8469}, {6.9158, 6.9166, 6.9190}, {3.5833, 3.5835, 3.5840}, and {2.2054, 2.2055, 2.2056}. For $n > 5$, we have that $|\max\{\phi_{n,L}(\ell), \phi_{n,L}(\lambda)\}/\phi_n - 1|$ and $|\min\{\phi_{n,U}(\ell), \phi_{n,U}(\lambda)\}/\phi_n - 1|$ are smaller than 10^{-4}.

We can then use the bounds on the eigenvalues to obtain bounds on the eigenvectors of V_D and V_D^{-1}. From Lemma 2 we have that

$$\gamma_n = \frac{g_n}{\left\|\Psi\left(\Lambda_\ell - \phi_{N-n+1}^{-1}I_N\right)^{-1}\Psi'x\right\|}, \qquad g_n = \Psi\left(\Lambda_\ell - \phi_{N-n+1}^{-1}I_N\right)^{-1}\Psi'x,$$

where $\Lambda_\ell = \mathrm{diag}(\ell_N, \ell_{N-1}, \ldots, \ell_1)$. Recall that the (i, j) element of Ψ is $\psi_{i,j}$. Let $g_{i,n}$ be the ith element of g_n, where

$$g_{i,n} = \sqrt{\frac{\rho(1-\rho)}{\sigma^2}} \sum_{k=1}^{N} \frac{\psi_{i,k}\psi_{N,k}}{\ell_{N-k+1} - \phi_{N-n+1}^{-1}}.$$

In order to provide bounds on $g_{i,n}$, we need to deal with the term $\ell_{N-k+1} - \phi_{N-n+1}^{-1}$. Notice that

$$\ell_{N-k+1} - \phi_{N-n+1}^{-1} = \lambda_k^{-1} - \phi_{N-n+1}^{-1} = \frac{\phi_{N-n+1} - \lambda_k}{\phi_{N-n+1}\lambda_k}.$$

Thus,

$$\gamma_{i,n} = \frac{g_{i,n}}{\left\| \Psi\left(\Lambda_\ell - \phi_{N-n+1}^{-1} I_N\right)^{-1} \Psi' x \right\|}, \qquad g_{i,n} = \sqrt{\frac{\rho(1-\rho)}{\sigma^2}} \sum_{k=1}^{N} \frac{\phi_{N-n+1}\lambda_k \cdot \psi_{i,k}\psi_{N,k}}{\phi_{N-n+1} - \lambda_k}.$$

However,

$$\max\{\phi_{N-n+1,L}(\ell), \phi_{N-n+1,L}(\lambda)\} - \lambda_k \le \phi_{N-n+1} - \lambda_k$$
$$\le \min\{\phi_{N-n+1,U}(\ell), \phi_{N-n+1,U}(\lambda)\} - \lambda_k,$$

and so long as the signs of the upper and lower bounds are the same, we can then bound the individual summands which comprise $g_{i,n}$. In some situations, these bounds are uninformative, but as shown in Figure B.1, for our case, they provide relatively tight bounds on the first three eigenvectors of V_D (especially for the first principal component). This is shown in the left chart. In the right chart, we show the scree plot along with the bounds
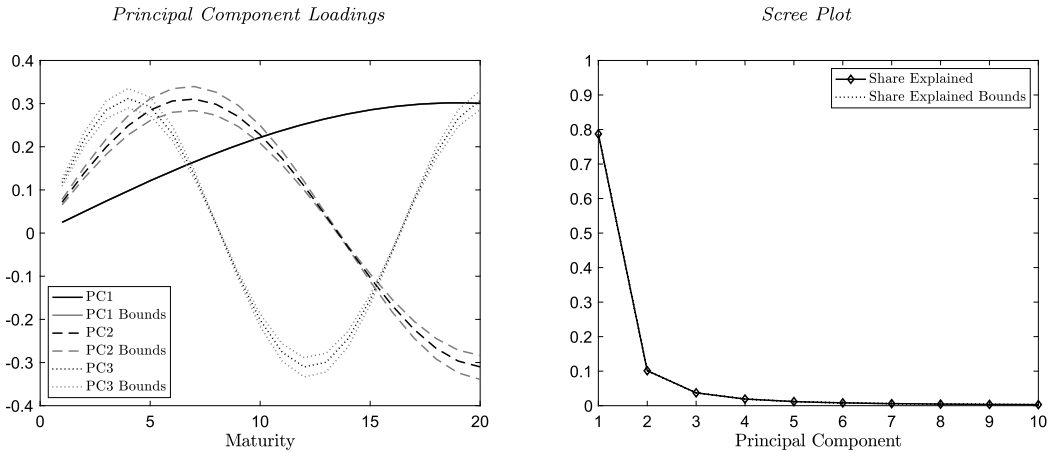

FIGURE B.1.—Eigenvalues and eigenvector bounds. This figure shows the output from principal component analysis applied to the variance-covariance matrix of difference returns shown in equation (12) for $\rho = 0.99$ and maximum maturity $N = 20$ based on Lemma 2 in the paper. The left chart shows the principal component loadings for the first three principal components of V_D along with upper and lower bounds; the right chart shows the scree plot for the first ten principal components along with upper and lower bounds.

on the explained variation of each principal component based on the eigenvalue bounds given in this section. These bounds are so tight that they are imperceptible based on a visual inspection of the chart.

APPENDIX C: ADDITIONAL EMPIRICAL EVIDENCE

In this appendix, we provide additional empirical evidence on properties of the term structure. In Figure 1 in the paper, we presented results derived from traded prices of securities based on Eurodollar futures prices.[1] Figure 1 illustrates that these data have strong local correlation aligning with the approximation results introduced in Lemma 2 in the paper. However, there are other traded fixed-income securities which have different local correlation structure in their difference returns. Despite this, as we show below, the excess returns have strikingly similar properties.

As an alternative data set, we use coupon STRIPS prices of U.S. Treasury securities with quarterly maturities (see the next section for data description). Figure C.1 plots the time-series dynamics of excess returns and difference returns based on STRIPS data, which may be compared to the top two charts of Figure 1 for Eurodollar futures in the paper. Excess returns exhibit a pronounced commonality across maturities for both data sets, whereas difference returns for STRIPS display less structured co-movement than those of Eurodollars; however, they still clearly move together throughout the sample.

Figure C.2 shows that the local correlation structure of excess returns is broadly similar across the two data sets in our sample. Observe that there is some dependence in difference returns across maturities (as in Lemma 2), which is amplified and made uniform by the cross-sectional summation moving from difference returns to excess returns (Figures 2 and 4). In particular, note that the solid line in each chart is nearly identical
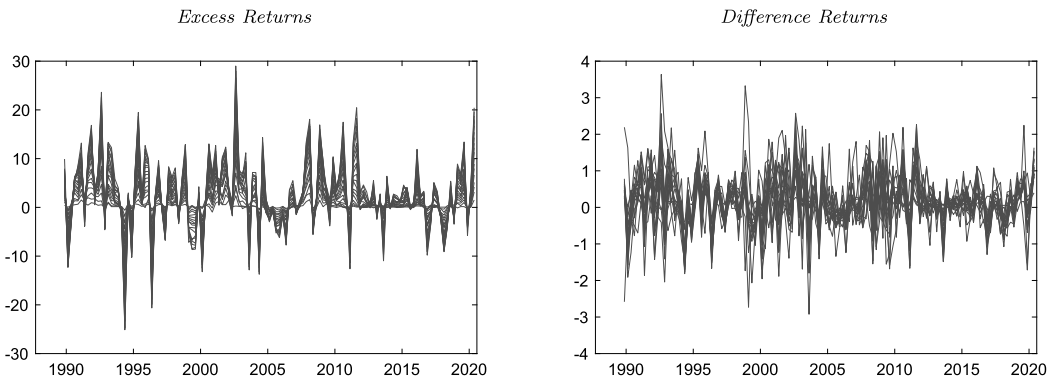

FIGURE C.1.—STRIPS data. The figure shows the time-series dynamics of STRIPS excess bond returns (left chart) and difference returns (right chart) for maturities up to 20 quarters (in percent, annualized). The sample period is 1989Q3–2020Q2.

---

[1]It is important that we perform our empirical assessments using unsmoothed curves, as parametrically fitted curves enhance the local correlation of observations with nearby maturities and further exacerbate the issues highlighted by our theoretical analysis. More generally, Cochrane and Piazzesi (2008) raised concerns of using parametrically fitted yield curves for empirical research. For this reason, we use prices based on directly tradable securities that are not subjected to statistical smoothing, which necessarily strengthens local dependence.

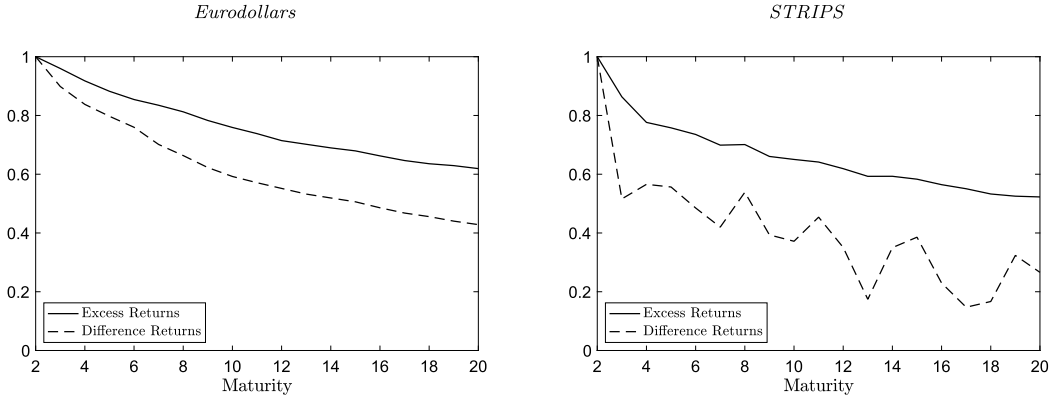*Eurodollars*   *STRIPS*

FIGURE C.2.—Correlation structure. This figure shows the Spearman's correlation coefficient between $rx_t^{(2)}$ and $rx_t^{(n)}$ (solid line), and $dr_t^{(2)}$ and $dr_t^{(n)}$ (dashed line) for $n \geq 2$. The left chart displays the results based on Eurodollar futures (1992Q3–2020Q2). The right chart displays the results based on STRIPS (1989Q3–2020Q2).

despite difference returns for Eurodollar futures behaving very differently than those for STRIPS.

It is instructive to further investigate the properties of these data by examining different transformations. Table C.I reports the explained variation from PCA applied to various yield curve objects for the two data sets. In addition to excess returns $rx_t^{(n)}$, holding-period returns $r_t^{(n)}$, and difference returns $dr_t^{(n)}$, we also include two other weakly serially correlated variables: yield changes, $\Delta y_t^{(n)} \equiv y_t^{(n)} - y_{t-1}^{(n)}$, and changes in forward rates, $\Delta f_t^{(n)} \equiv f_t^{(n)} - f_{t-1}^{(n)}$. Note that these two variables are closely related to returns and difference returns, respectively; for example, equation (6) implies that $dr_t^{(n)} = -(f_t^{(n-1)} - f_{t-1}^{(n)})$.

TABLE C.I

EXPLAINED VARIATION OF ORDERED PRINCIPAL COMPONENTS.

	Panel A: Eurodollar Futures					Panel B: STRIPS				
	$rx_t^{(n)}$	$r_t^{(n)}$	$\Delta y_t^{(n)}$	$\Delta f_t^{(n)}$	$dr_t^{(n)}$	$rx_t^{(n)}$	$r_t^{(n)}$	$\Delta y_t^{(n)}$	$\Delta f_t^{(n)}$	$dr_t^{(n)}$
1	98.366	95.684	93.467	89.375	88.782	97.818	93.097	90.419	41.692	51.661
2	1.5687	3.9368	6.0781	9.3719	9.7219	1.7276	6.1477	5.9377	12.054	9.0558
3	0.0521	0.3530	0.4101	0.8632	0.9767	0.1250	0.4545	0.7193	10.565	6.5757
4	0.0090	0.0210	0.0353	0.1450	0.3791	0.0610	0.0579	0.6092	9.6273	5.2696
5	0.0022	0.0028	0.0049	0.0996	0.0638	0.0483	0.0431	0.5572	6.4318	4.2994
6	0.0010	0.0017	0.0019	0.0534	0.0378	0.0345	0.0342	0.3560	4.4863	3.7229
7	0.0003	0.0006	0.0015	0.0356	0.0122	0.0308	0.0249	0.3067	3.8897	3.0808
8	0.0001	0.0001	0.0006	0.0310	0.0104	0.0263	0.0232	0.2405	3.5403	2.5733
9	0.0000	0.0001	0.0002	0.0110	0.0060	0.0239	0.0207	0.1680	2.1984	2.2322
10	0.0000	0.0000	0.0001	0.0067	0.0033	0.0186	0.0180	0.1439	1.5696	1.9715

Note: The table shows the explained variation (in %) for the ordered principal components for various term structure objects. The data used in Panel A are based on Eurodollar futures prices with quarterly maturities up to 20 quarters and sample period 1992Q3–2020Q2. The data used in Panel B are based on STRIPS prices with quarterly maturities of up to 20 quarters and sample period 1989Q3–2020Q2.

However, they do not share the appealing statistical properties and economic interpretation of returns.[2]

For both Eurodollar and STRIPS data, the variables based on overlapping maturity-ordered partial sums—excess returns, returns, and yield changes—appear to exhibit strong low-dimensional factor structure. For example, the first principal component for excess returns explains around 98% of the total variation for both data sets. By contrast, difference returns based on STRIPS data appear to be characterized by one dominant factor, which accounts for only 51.7% of the variation, and numerous weaker factors requiring 10 factors to reach 90% of the explained variation. The time-series change in forward rates, which are also not based on overlapping partial sums, follows a similar pattern although the percentage of explained variation is larger for Eurodollar data where the degree of local correlation is larger. For Eurodollar difference returns, the first three principal components still account for 99.5% of the explained variation. But while the contribution of the remaining factors is fairly small, the ratios of adjacent higher-order eigenvalues for difference returns appear range-bound, suggesting that they contain meaningful incremental information.

Finally, Figure C.3 shows the first three principal component loadings for excess returns and difference returns based on the STRIPS data. The loadings on the difference returns (right chart) do not exhibit the structured properties that we observed for Eurodollars in Figure 1 of the paper. Despite this, in Table C.I, we saw that the explained variation for the first three principal components of returns based on either data set were almost identical and in excess of 99.5%. The left chart of Figure C.3 confirms this observation and shows that the principal component loadings for excess returns are remarkably similar as well (see Figure 1). Taken all together, the empirical results in this section are consistent with the main message of the paper that characterizing the minimal dimension of the term structure of interest rates proves to be extremely challenging.
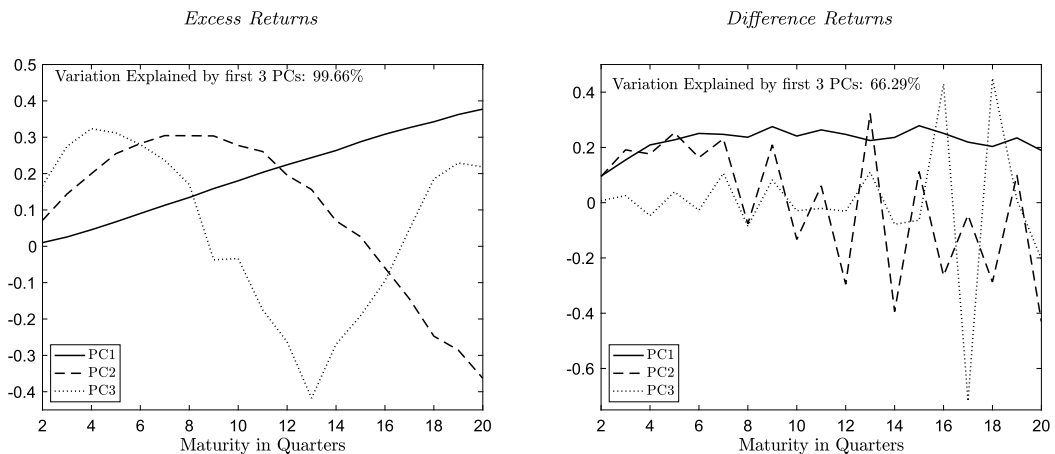

FIGURE C.3.—Principal component loadings of STRIPS data. The figure shows the first three principal component loadings for excess returns (left chart) and difference returns (right chart) for maturities up to 20 quarters (in percent, annualized). The sample period is 1989Q3–2020Q2.

---

[2]Note that yield and forward rate changes have a clear negative drift as a result of the sustained decline in overall yield levels over the last 40 years.

APPENDIX D: DATA DESCRIPTION

This appendix provides a more detailed description of the data sets used in the paper and in Appendix C.

Eurodollar Futures. Eurodollar futures are futures contracts with final price based on the three-month LIBOR interest rate at the expiration date.[3] We obtain daily closing prices of Eurodollar futures from the CME for the sample from 1992Q3 to 2016Q4 and from Bloomberg for the sample from 2017Q1 to 2020Q2. To construct a zero-coupon yield curve directly from traded futures prices, we take the settlement value of the March, June, September, and December quarterly contracts on settlement dates for maturities up to five years. We use the implied yield curve (100 minus the futures price) to construct a theoretical zero-coupon yield curve from which we compute forwards, returns, excess returns, and difference returns using the definitions introduced in Section 2 of the paper.

STRIPS (Separate Trading of Registered Interest and Principal of Securities). STRIPS are separately traded zero-coupon securities derived from the coupon or principal payments of a Treasury note or bond. We obtain daily observations for coupon STRIPS bid prices of notes and bonds from the Wall Street Journal from 1989Q3 to 1997Q4 and from Street Software Technology Inc. from 1998Q1 to 2020Q2. To construct a quarterly series, we use the daily price observations at the middle of the 2nd month of the quarter to align the maturity and time interval. We then construct forwards, returns, excess returns, and difference returns using the definitions introduced in Section 2 of the paper. For a more detailed description of the data, see Sack (2000) as well as Appendix C in Crump and Gospodinov (2019).

REFERENCES

BIKBOV, R., AND M. CHERNOV (2011): "Yield Curve and Volatility: Lessons From Eurodollar Futures and Options," *Journal of Financial Econometrics*, 9 (1), 66–105. [7]

BURGHARDT, G. (2003): *The Eurodollar Futures and Options Handbook*. McGraw-Hill. [7]

COCHRANE, J., AND M. PIAZZESI (2008): "Decomposing the Yield Curve," Working paper. [4]

CRUMP, R. K., AND N. GOSPODINOV (2019): "Deconstructing the Yield Curve," Staff Report 884, Federal Reserve Bank of New York. [7]

IPSEN, I., AND B. NADLER (2009): "Refined Perturbation Bounds for Eigenvalues of Hermitian and Non-Hermitian Matrices," *SIAM Journal on Matrix Analysis and Applications*, 31 (1), 40–53. [1,2]

PIAZZESI, M., AND E. T. SWANSON (2006): "Futures Prices as Risk-Adjusted Forecasts of Monetary Policy," Working Paper 2006-23, Federal Reserve Bank of San Francisco. [7]

SACK, B. (2000): "Using Treasury STRIPS to Measure the Yield Curve," Finance and Economics Discussion Series 2000-42, Federal Reserve Board. [7]

[3]Burghardt (2003) provided a comprehensive summary of the Eurodollar futures market. For other studies which use Eurodollar futures data see, for example, Piazzesi and Swanson (2006) and Bikbov and Chernov (2011).